JACS Au
AN OPEN ACCESS JOURNAL OF THE AMERICAN CHEMICAL SOCIETY

pubs.acs.org/jacsau

Letter

Precision Deuteration Using Cu-Catalyzed Transfer Hydrodeuteration to Access Small Molecules Deuterated at the Benzylic Position

Samantha E. Sloane, Zoua Pa Vang, Genevieve Nelson, Lihan Qi, Reilly E. Sonstrom, Isabella Y. Alansari, Kiera T. Behlow, Brooks H. Pate,* Sharon R. Neufeldt,* and Joseph R. Clark*

Cite This: *JACS Au* 2023, 3, 1583−1589

Read Online

ACCESS | Metrics & More | Article Recommendations | Supporting Information

ABSTRACT: A highly regio- and chemoselective Cu-catalyzed aryl alkyne transfer hydrodeuteration to access a diverse scope of aryl alkanes precisely deuterated at the benzylic position is described. The reaction benefits from a high degree of regiocontrol in the alkyne hydrocupration step, leading to the highest selectivities reported to date for an alkyne transfer hydrodeuteration reaction. Only trace isotopic impurities are formed under this protocol, and analysis of an isolated product by molecular rotational resonance spectroscopy confirms that high isotopic purity products can be generated from readily accessible aryl alkyne substrates.

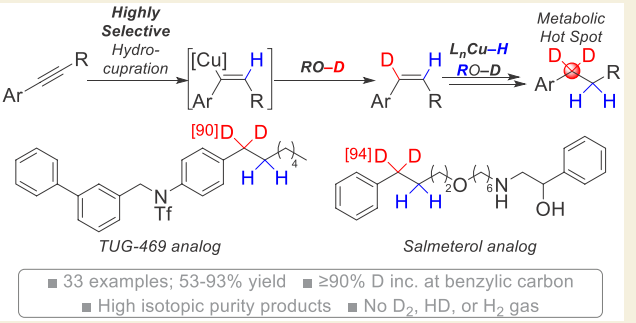

KEYWORDS: *deuterium, precision deuteration, rotational spectroscopy, copper catalysis, hydrodeuteration*

Selectively deuterated small molecules are utilized across many disciplines of science, especially chemistry. In addition to studying the stereochemical course of microbiological or enzymatic reactions,[1−4] they serve as probes to study reaction mechanisms, perform kinetic isotope effect studies, and elucidate biosynthetic pathways.[5−8] They are also used as internal standards for high-resolution mass spectrometry.[1,9,10] Selectively deuterated small molecules are becoming increasingly important in the development of novel pharmaceuticals,[11−14] and the FDA approval of deutetrabenazine in 2017 sparked a renewed interest in the development of precisely deuterated small-molecule drugs.[15] As of 2019, there were 20 deuterated drugs in clinical development.[11] Significantly, deuterated bioisosteres that are designed to increase the half-life of a drug or divert a specific metabolic pathway hold significant potential as safer therapeutics.[11−13,16,17] The high frequency of metabolic oxidation occurring at a benzylic position in drug molecules makes this an important site for precise or targeted deuteration. However, unique synthetic challenges exist for developing highly selective reactions for benzylic deuteration.

Hydrogen isotope exchange (HIE) reactions efficiently incorporate deuterium into aliphatic bonds of small molecules,[18−22] but selectivity challenges in these reactions make it difficult to control the exact quantity and placement of deuterium within the molecule, especially when targeting benzylic deuteration.[19,23−26] From a drug discovery perspective, deuterium-labeled drug candidates that are free of isotopic impurities are desirable since misdeuterated or underdeuterated isotopic impurities can lead to compromised pharmacokinetics.[27,28] However, due to the similar physical properties of deuterium relative to hydrogen, isotopic mixtures are inseparable using common purification techniques. As such, it is critical to develop deuteration methods that perform with higher precision than HIE reactions.

Traditionally, alkyl aromatics containing two deuterium atoms at the benzylic position are accessed via de novo syntheses. Direct access is commonly achieved via a deoxygenative deuteration of aryl carbonyl compounds, where relatively forcing conditions are sometimes required, thereby limiting reaction scope.[29−31] Even modern and more mild protocols for deoxygenative deuteration can lead to significant levels of inseparable isotopic impurities and remain deficient for N-heterocycle or amine-containing substrates (Scheme 1a).[32] Alternatively, highly selective single-electron-transfer carbonyl reductive deuterations exist for accessing compounds deuterated at the benzylic position, but only for the synthesis of α,α-dideuteriobenzyl alcohols (Scheme 1b).[33−35] Recognizing the importance of complete deuteration at only the target site for pharmaceutical applications, we

Received: January 31, 2023
Revised: May 8, 2023
Accepted: May 9, 2023
Published: May 17, 2023

https://doi.org/10.1021/jacsau.3c00053
JACS Au 2023, 3, 1583−1589

Scheme 1. Synthesis of Small Molecules Perdeuterated at the Benzylic Position

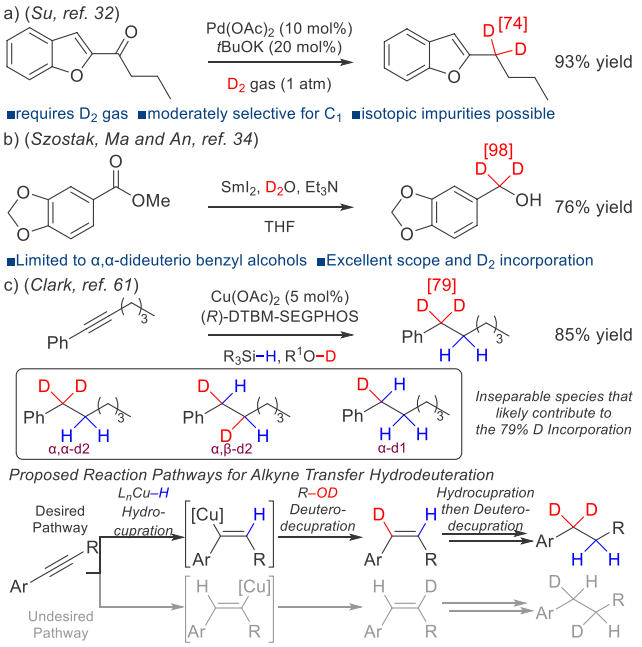

sought to develop a mild and general reaction for the selective synthesis of molecules precisely deuterated at the benzylic position. Importantly, the reaction must be compatible with functionality commonly found in small-molecule drugs such as amines, O-, S-, or N-containing heterocycles, esters, and halogens.[36,37]

Catalytic transfer hydrodeuteration has significant potential for making selectively deuterated alkanes.[38−43] Inspired by highly selective processes for [Cu−H]-catalyzed alkene[44−48] and alkyne[49−60] hydrofunctionalizations, our group reported an aryl alkyne transfer hydrogenation and deuteration reaction catalyzed by $Cu(OAc)_2$ and DTBM-SEGPHOS.[61] In that study, the protocol was modified to investigate an unprecedented internal aryl alkyne transfer hydrodeuteration process, albeit with moderate levels of deuterium incorporation (Scheme 1c). Despite the efficiency of the reaction, several underlying selectivity challenges surfaced. To prepare compounds containing exactly two deuterium atoms at the benzylic position with high levels of isotopic purity (i.e., the isolated product composition consists of ≥90% of the desired isotopomer), a high degree of regiocontrol is required for both the alkyne and alkene hydrocupration steps. Since aryl alkene hydrocupration occurs in a highly regioselective manner,[62,63] likely because of the thermodynamic favorability of a benzylic copper intermediate, we turned our focus to understanding the factors influencing regioselectivity for internal aryl alkyne hydrocupration.

In the alkyne transfer hydrodeuteration reaction (Scheme 1c), we believe that there are at least three isotopic species that contribute to the modest 79% benzylic deuterium incorporation. Despite this reaction outcome, only the α,α-d2 isotopomer is useful for studies aimed at modulating oxidative processes at the benzylic carbon. Therefore, in an optimal setting where alkene hydrocupration is completely regioselective, a minimum 9:1 r.r. for alkyne hydrocupration must be achieved for the reaction product to contain a synthetically useful ≥90% composition of the α,α-d2 isotopomer.

A survey of previously reported [Cu−H]-catalyzed alkyne hydrofunctionalization reactions reveals that aryl- or alkyl-substituted terminal alkynes undergo hydrocupration with anti-Markovnikov regioselectivity as a result of Cu insertion at the less sterically hindered terminal position.[49−53] However, the increased steric hindrance of an internal aryl alkyne leads to a modest preference for the product resulting from Cu insertion α to the arene.[57,64−66] Prior density functional theory (DFT) calculations suggest that the demanding steric environment of the aryl substituent is counterbalanced by energetic stabilization provided by the overlap of the empty Cu d orbital with the aryl π system when Cu inserts at the α-carbon.[67] With the goal of improving the regioselectivity of alkyne hydrocupration to achieve a minimum 9:1 r.r. for internal aryl alkyne hydrocupration, we sought to exploit these interactions through ligand choice.

We began by studying the outcome of the alkyne hydrodeuteration at early time points using substrate **1**. By doing so, the α- and β-deuterated styrene products *E*/*Z*-**2** and *E*/*Z*-**3** could be observed, resulting from semireduction of **1** (Scheme 2). Given the prevalence of NHC−Cu catalysts in

Scheme 2. Aryl Alkyne Hydrocupration Regioselectivity Studies

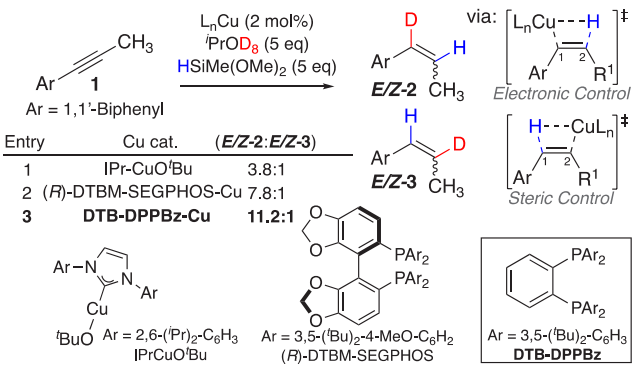

alkyne hydrofunctionalization reactions,[57,64−66] the IPr−Cu catalyst was evaluated first and found to be moderately regioselective for alkyne hydrometalation (3.8:1 r.r.; entry 1). Evaluating DTBM-SEGPHOS, the ligand that we previously evaluated for alkene and alkyne transfer hydrodeuteration and Buchwald and co-workers used for alkyne hydroamination,[56,61] led to a near doubling of the hydrocupration regioselectivity (7.8:1 r.r.; entry 2). However, switching to DTB-DPPBz, a ligand previously demonstrated by our research group to support a highly regioselective alkene transfer hydrodeuteration reaction,[62,68] led to the most significant increase in the alkyne hydrocupration regioselectivity (11.2:1 r.r.; entry 3).

Having identified a ligand that induces high regioselectivity for both alkyne and alkene hydrocupration, we next turned to studying the full reduction of **4a** to prepare high-purity α,α-dideuterated aryl alkanes (Scheme 3). Gratifyingly, using DTB-DPPBz, dimethoxy(methyl)silane, and isopropanol-d_8 along with performing the reaction in THF at 40 °C results in a high yield and deuterium incorporation for desired product **5a** (97% yield, 95% D inc.; see the Supporting Information (SI) for optimization studies).

The reaction scope of internal aryl alkynes for Cu-catalyzed transfer hydrodeuteration was evaluated. The desired α,α-d2 isotopomer was accessed from a phenylhexyne substrate and arenes substituted with one or two methyl groups (Scheme 3,

https://doi.org/10.1021/jacsau.3c00053
JACS Au 2023, 3, 1583−1589

Scheme 3. Aryl Alkyne Substrate Scope

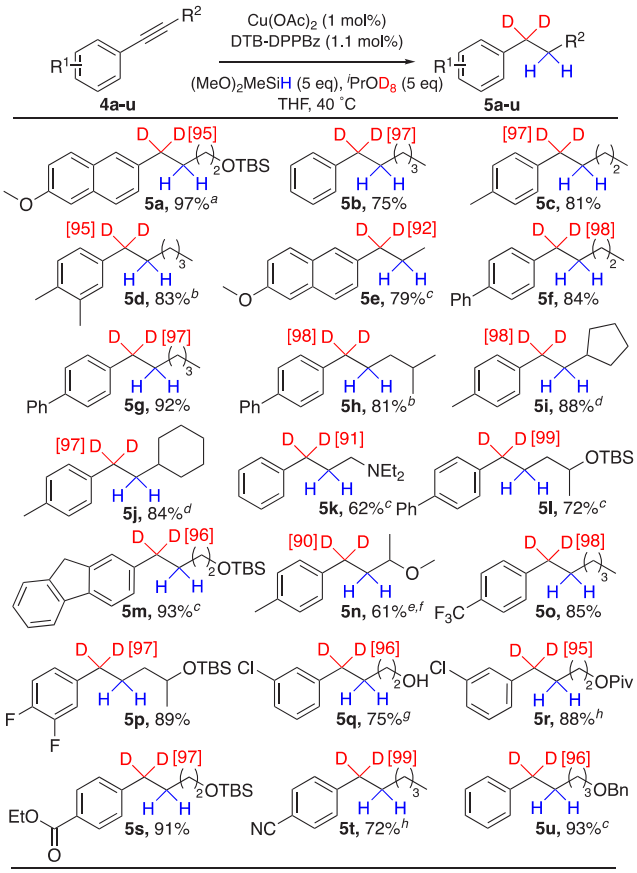

[a]Using *i*PrOD instead of *i*PrOD$_8$ results in a 91% isolated yield of **5a** with 95% D inc. [b]5 mol % Cu(OAc)$_2$ and 5.5 mol % DTB-DPPBz were used. [c]2 mol % Cu(OAc)$_2$ and 2.2 mol % DTB-DPPBz were used. [d]Poly(methylhydrosiloxane) (5 equiv) was used. [e]3 mol % Cu(OAc)$_2$ and 3.3 mol % DTB-DPPBz were used. [f]6 equiv of (MeO)$_2$MeSiH was used. [g]Isolated yield over two steps after deprotection of the TBS group. [h]The reaction was performed at 5 °C.

5b–**5d**, 75–83% yield). These results compare favorably to our prior studies depicted in Scheme 1c.[61] Effects from variation of the alkane chain length were studied, and excellent yields were obtained with a propyne, pentyne, or hexyne chain (**5e**–**5g**, 79–92% yield). Using isobutyl-, cyclopentyl-, or cyclohexyl-substituted alkyne substrates also led to highly regioselective reactions (**5h**–**5j**, 81–88% yield). Lewis basic nitrogen functionality is compatible with the reaction (**5k**, 62% yield), while alcohol-containing substrates required a protecting group to avoid competitive protodecupration pathways (**5l**–**5n**, 61–93% yield). Halogenated substrates along with aryl alkyne substrates containing reducible functionality such as an ethyl ester, cyano, or benzyl ether group undergo chemoselective alkyne transfer hydrodeuteration (**5o**–**5u**, 72–93% yield). When ketone or aryl bromide functionality was present, the reaction was not chemoselective for only alkyne transfer hydrodeuteration. The ketone was reduced to a silyl ether, and the aryl bromide substrate only reached partial conversion with trace reductive debromination product detected (see the SI for details).

Due to their prevalence in small-molecule drugs, heterocycle-containing aryl alkyne substrates were evaluated for selective Cu-catalyzed alkyne transfer hydrodeuteration. Quinoline, Ts-protected azaindole, Ts-protected carbazole, Ts-protected indole, and thiophene aryl alkynes underwent highly selective transfer hydrodeuteration (Scheme 4, **7a**–**7e**,

Scheme 4. Heterocycle and Complex Small Molecule Scope

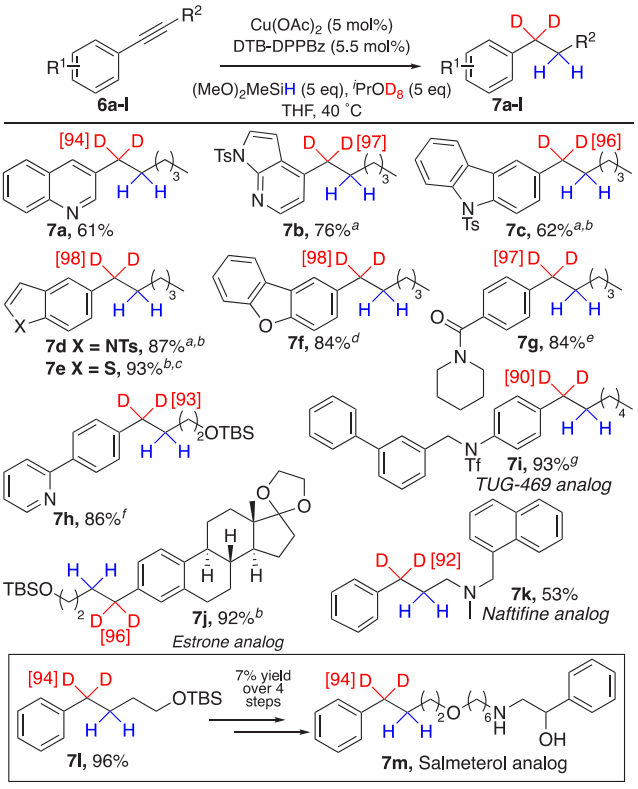

[a]The reaction was performed at 60 °C. [b]6 equiv of (MeO)$_2$MeSiH was used. [c]1 mol % Cu(OAc)$_2$ and 1.1 mol % DTB-DPPBz were used. [d]2 mol % Cu(OAc)$_2$ and 2.2 mol % DTB-DPPBz were used. [e]6 equiv of *i*PrOD$_8$ was used. [f]6.8 mol % Cu(OAc)$_2$, 7.4 mol % DTB-DPPBz, 8.1 equiv of (MeO)$_2$MeSiH, and 6.8 equiv of *i*PrOD$_8$ were used. [g]5.2 mol % Cu(OAc)$_2$, 5.7 mol % DTB-DPPBz, 5.2 equiv of (MeO)$_2$MeSiH, and 5.2 equiv of *i*PrOD$_8$ were used.

61–93% yield), along with dibenzofuran- or amide-substituted alkynes (**7f** and **7g**, 84% yield). Even substitution of a phenyl alkyne with a pyridine, one of the most prevalent heterocycles in small-molecule drugs,[36,37] results in a high yield of the desired deuterated product (**7h**, 86% yield).

The synthesis of four complex bioactive molecules exclusively deuterated at the benzylic position was performed. This included late-stage transfer hydrodeuterations of alkyne-containing derivatives of TUG-469,[69] estrone, and naftifine.[70] Each reaction proceeded with high deuteration efficiency (**7i**–**7k**, 53–93% yield, ≥90% D inc.). Lastly, **7l** was accessed in excellent yield and deuterium incorporation. This deuterated building block was then used to synthesize salmeterol analog **7m**, where deuterium is exclusively contained at the benzylic position prone to metabolic oxidation.[71]

Molecular rotational resonance (MRR) spectroscopy is an emerging technology for the characterization and quantification of isotopically labeled compounds. Instruments for rotational spectroscopy have exceptionally high spectral resolution so that the different isotopic species can be observed without spectral overlap. This presents a practical solution to some challenges in NMR spectroscopy where isotopologues and isotopomers in product mixtures may share

https://doi.org/10.1021/jacsau.3c00053
JACS Au 2023, 3, 1583–1589

deuterium substitution at the same atom so that several isotopic species contribute to the same $^{1}H/^{2}H$ resonance.[62,72]

MRR analysis was performed on the reaction products of the phenylhexyne substrate, **4b**. The analysis was performed in two steps (Scheme 5). Using the nonselectively deuterated sample

Scheme 5. Analysis by Molecular Rotational Resonance

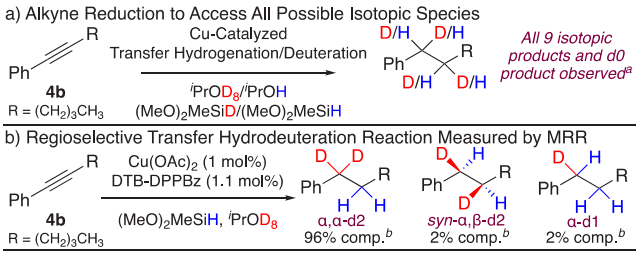

[a]See the SI for all isotopic products. [b]Denotes the average percent composition of isolated product from two runs.

of Scheme 5a, the spectroscopic signatures of all 10 possible species associated with hydrogen and/or deuterium insertion at any of the α- or β-benzylic CH positions were obtained using a broadband chirped-pulse Fourier transform microwave spectrometer (see the SI for analysis details).[73] The composition of the reaction mixture from the selective deuteration process of Scheme 5b was analyzed using an IsoMRR instrument that employs cavity-enhanced Fourier transform microwave spectroscopy[74] to reduce measurement time and sample consumption. Two separate sample preparations were analyzed and found to have nearly identical compositions. The results are summarized in Scheme 5b. Only two isotopic impurities were detected above the measurement threshold of 0.5%. Note that the homochiral and heterochiral diastereomers for the α,β-d2 species have different rotational spectra and are easily distinguished in the MRR analysis. The observation of just the heterochiral diastereomer is consistent with a reaction mechanism that favors *syn* addition of the [Cu−H] in both the alkyne and alkene addition steps.[61,62]

We performed DFT calculations to understand the enhanced alkyne hydrocupration regioselectivity observed with the DTB-DPPBz ligand relative to the DTBM-SEGPHOS ligand. For the addition of (DTB-DPPBz)CuH to 1-phenylpropyne, Cu favors insertion α to the arene by 5.0 kcal/mol at the level of theory used (Figure 1a; see the SI for the full energy diagram of this step). In contrast, (DTBM-SEGPHOS)CuH is unselective, showing a slight preference for insertion of Cu β to the arene. These predictions are qualitatively consistent with the experimental observation that DTB-DPPBz promotes higher selectivity for α-deuteration than does DTBM-SEGPHOS.

The origin of the increased selectivity with DTB-DPPBz relates to orbital mixing between the ligand and Cu during the favored transition state **TS8a**. In both **TS8a** and **TS8b**, the five-membered cupracycle of (DTB-DPPBz)CuH adopts the same "envelope" conformation, and the substrate phenyl group points toward the less hindered *endo* face of the cupracycle (Figure 1b). In this geometry, two *P*-aryl groups are pseudoaxial with respect to the five-membered cupracycle. When the hydride is on the *exo* face of the cupracycle as in **TS8a**, the π^* orbitals of these aryl groups can mix with a metal-centered p-type orbital to form the LUMO (Figure 1c). This mixing lowers the energy of the lowest unoccupied metal-

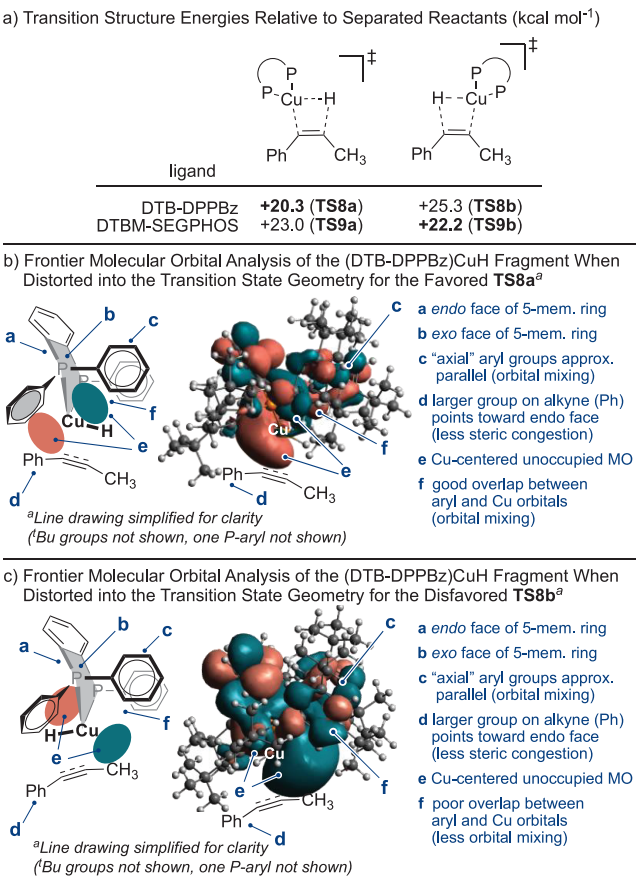

d) Orbital Energies for (DTB-DPPBz)CuH and (DTBM-SEGPHOS)CuH

entry	complex	MO	MO energy (eV)
1	**(DTB-DPPBz)**CuH (relaxed)	LUMO+1	-0.916
2	**(DTB-DPPBz)**CuH (distorted α)	LUMO	**-1.007**
3	**(DTB-DPPBz)**CuH (distorted β)	LUMO+1	**-0.835**
4	**(DTBM-SEGPHOS)**CuH (relaxed)	LUMO	-0.931
5	**(DTBM-SEGPHOS)**CuH (distorted α)	LUMO	**-0.903**
6	**(DTBM-SEGPHOS)**CuH (distorted β)	LUMO	-0.936

Figure 1. DFT analysis of alkyne hydrocupration with (DTB-DPPBz)CuH.

centered MO of (DTB-DPPBz)CuH when it is distorted into the **TS8a** geometry (Figure 1d, compare entries 1 and 2). The low-energy LUMO facilitates electron donation from the alkyne to copper. However, when the hydride is on the *endo* face of the cupracycle as in **TS8b**, there is poor overlap between ligand and metal orbitals, and the LUMO energy is actually higher in the distorted geometry (entry 3) compared to the ground state. The conformational preference of the five-membered cupracycle is critical to the difference between **TS8a** and **TS8b**. For (DTBM-SEGPHOS)CuH, Cu is part of a seven-membered ring, which does not result in the same orbital mixing effect. Indeed, the LUMO energy of (DTBM-SEGPHOS)CuH is slightly raised by distortion into the **TS9a** geometry and not significantly affected in **TS9b** (entries 4−6).

In conclusion, the first highly regioselective transfer hydrodeuteration reaction of aryl alkynes is reported across a broad substrate scope. DFT calculations are consistent with experimental findings and reveal that the high regioselectivity observed in the alkyne hydrocupration step can be attributed to enhanced electronic interactions between the substrate and (DTB-DPPBz)CuH complex. We anticipate that this reaction and the spectroscopic techniques employed to quantify and

https://doi.org/10.1021/jacsau.3c00053
JACS Au 2023, 3, 1583−1589

characterize the isotopic species will be useful in the development of precisely deuterated small molecules for pharmaceutical applications.

General Procedure for Cu-Catalyzed Transfer Hydrodeuteration

In a N_2-filled glovebox, DTB-DPPBz (0.0110 equiv), $Cu(OAc)_2$ (0.200 M solution in THF, 0.0100 equiv), and THF were added to an oven-dried 2 dram vial followed by dropwise addition of dimethoxy(methyl)silane (185 μL, 1.50 mmol, 5.00 equiv) or poly(methylhydrosiloxane) (100 μL, 1.50 mmol, 5.00 equiv based on Si−H). A color change from green/blue to yellow was observed while stirring for 15 min. In a separate oven-dried 1 dram vial were added the alkyne substrate (0.300 mmol, 1.00 equiv), THF (0.150 mL), and 2-propanol-d_8 (115 μL, 1.50 mmol, 5.00 equiv). The solution in the 1 dram vial was added dropwise over 20 s to the 2 dram vial. The total volume of THF was calculated based on having a final reaction concentration of 1 M based on the alkyne substrate. The 2 dram vial was capped with a red pressure relief cap, taken out of the glovebox, and stirred for the respective time at the appropriate temperature, at which point the reaction was filtered through a 1″ silica plug with 50 mL of Et_2O or CH_2Cl_2 followed by 50 mL of Et_2O or CH_2Cl_2 to elute the remaining product into a 200 mL round-bottom flask. After removal of the solvent by rotary evaporation, the crude product was isolated by flash column chromatography.

■ ASSOCIATED CONTENT

Supporting Information

The Supporting Information is available free of charge at https://pubs.acs.org/doi/10.1021/jacsau.3c00053.

General information; procedures for transfer hydrodeuteration and synthesis of starting materials; ^1H, ^2H, and ^{13}C NMR spectra and HRMS and IR data for all newly characterized products; molecular rotational resonance spectroscopy data in Scheme 5; computational study details (PDF)

Cartesian coordinates (XYZ)

■ AUTHOR INFORMATION

Corresponding Authors

Joseph R. Clark − *Department of Chemistry, Marquette University, Milwaukee, Wisconsin 53233-1881, United States;* orcid.org/0000-0002-3081-5732; Email: joseph.r.clark@marquette.edu

Sharon R. Neufeldt − *Department of Chemistry & Biochemistry, Montana State University, Bozeman, Montana 59717, United States;* orcid.org/0000-0001-7995-3995; Email: sharon.neufeldt@montana.edu

Brooks H. Pate − *Department of Chemistry, University of Virginia, Charlottesville, Virginia 22904-4319, United States;* orcid.org/0000-0002-6097-7230; Email: bp2k@virginia.edu

Authors

Samantha E. Sloane − *Department of Chemistry, Marquette University, Milwaukee, Wisconsin 53233-1881, United States*

Zoua Pa Vang − *Department of Chemistry, Marquette University, Milwaukee, Wisconsin 53233-1881, United States*

Genevieve Nelson − *Department of Chemistry & Biochemistry, Montana State University, Bozeman, Montana 59717, United States*

Lihan Qi − *Department of Chemistry, Marquette University, Milwaukee, Wisconsin 53233-1881, United States*

Reilly E. Sonstrom − *BrightSpec Inc., Charlottesville, Virginia 22903, United States*

Isabella Y. Alansari − *Department of Chemistry, Marquette University, Milwaukee, Wisconsin 53233-1881, United States*

Kiera T. Behlow − *Department of Chemistry, Marquette University, Milwaukee, Wisconsin 53233-1881, United States*

Complete contact information is available at: https://pubs.acs.org/10.1021/jacsau.3c00053

Funding

Research reported in this publication was supported by the National Institute of General Medical Sciences of the National Institutes of Health under Award R35 GM147441-01. The content is solely the responsibility of the authors and does not necessarily reflect the official views of the National Institutes of Health. J.R.C. also acknowledges the donors of the American Chemical Society Petroleum Research Fund (65384-DNI1) for partial support of this research and Marquette University for financial support in the form of startup funds. MRR analysis of the isotopic impurities was performed with support from the National Science Foundation Chemical Measurement and Imaging Program under Grant NSF-1904686. Calculations were performed on Expanse at SDSC through XSEDE (CHE-170089), which was supported by NSF (ACI-1548562). HRMS was performed by the University at Buffalo Instrument Center (NIH S10 RR029517, NSF CHE-1919594).

Notes

The authors declare the following competing financial interest(s): B.H.P. has founders equity in BrightSpec, which commercializes applications of rotational spectroscopy in chemical analysis.

■ ACKNOWLEDGMENTS

I.Y.A. is grateful for a 2021 Eugene Kroeff Summer Research Fellowship. Z.P.V. thanks Marquette University Department of Chemistry for an Eisch Fellowship and MGS Summer Fellowship and Marquette University for the Schmidt Fellowship. S.E.S. thanks Marquette University for the O'Brien Fellowship.

■ REFERENCES

(1) Atzrodt, J.; Derdau, V.; Kerr, W. J.; Reid, M. Deuterium- and Tritium-Labelled Compounds: Applications in the Life Sciences. *Angew. Chem., Int. Ed.* **2018**, *57*, 1758−1784.

(2) Schwab, J. M. Stereochemistry of an enzymic Baeyer-Villiger reaction. Application of deuterium NMR. *J. Am. Chem. Soc.* **1981**, *103*, 1876−1878.

(3) Lüthy, J.; Rétey, J.; Arigoni, D. Asymmetric Methyl Groups: Preparation and Detection of Chiral Methyl Groups. *Nature* **1969**, *221*, 1213−1215.

(4) White, R. E.; Miller, J. P.; Favreau, L. V.; Bhattacharyya, A. Stereochemical dynamics of aliphatic hydroxylation by cytochrome P-450. *J. Am. Chem. Soc.* **1986**, *108*, 6024−6031.

(5) Simmons, E. M.; Hartwig, J. F. On the Interpretation of Deuterium Kinetic Isotope Effects in C-H Bond Functionalizations by Transition-Metal Complexes. *Angew. Chem., Int. Ed.* **2012**, *51*, 3066−3072.

(6) Meek, S. J.; Pitman, C. L.; Miller, A. J. M. Deducing Reaction Mechanism: A Guide for Students, Researchers, and Instructors. *J. Chem. Educ.* **2016**, *93*, 275−286.

(7) Gómez-Gallego, M.; Sierra, M. A. Kinetic Isotope Effects in the Study of Organometallic Reaction Mechanisms. *Chem. Rev.* **2011**, *111*, 4857−4963.

(8) Klinman, J. P. A new model for the origin of kinetic hydrogen isotope effects. *J. Phys. Org. Chem.* **2010**, *23*, 606−612.
(9) Qin, M.; Qiao, H.-q.; Yuan, Y.-j.; Shao, Q. A quantitative LC-MS/MS method for simultaneous determination of deuvortioxetine, vortioxetine and their carboxylic acid metabolite in rat plasma, and its application to a toxicokinetic study. *Anal. Methods* **2018**, *10*, 1023−1031.
(10) Iglesias, J.; Sleno, L.; Volmer, D. A. Isotopic Labeling of Metabolites in Drug Discovery Applications. *Curr. Drug Metab.* **2012**, *13*, 1213−1225.
(11) Pirali, T.; Serafini, M.; Cargnin, S.; Genazzani, A. A. Applications of Deuterium in Medicinal Chemistry. *J. Med. Chem.* **2019**, *62*, 5276−5297.
(12) Meanwell, N. A. Synopsis of Some Recent Tactical Application of Bioisosteres in Drug Design. *J. Med. Chem.* **2011**, *54*, 2529−2591.
(13) Gant, T. G. Using Deuterium in Drug Discovery: Leaving the Label in the Drug. *J. Med. Chem.* **2014**, *57*, 3595−3611.
(14) Nelson, S. D.; Trager, W. F. The Use of Deuterium Isotope Effects to Probe the Active Site Properties, Mechanism of Cytochrome P450-Catalyzed Reactions, and Mechanisms of Metabolically Dependent Toxicity. *Drug Metab. Dispos.* **2003**, *31*, 1481−1497.
(15) Schmidt, C. First deuterated drug approved. *Nat. Biotechnol.* **2017**, *35*, 493−494.
(16) Stepan, A. F.; Mascitti, V.; Beaumont, K.; Kalgutkar, A. S. Metabolism-guided drug design. *MedChemComm* **2013**, *4*, 631−652.
(17) Belleau, B.; Burba, J.; Pindell, M.; Reiffenstein, J. Effect of Deuterium Substitution in Sympathomimetic Amines on Adrenergic Responses. *Science* **1961**, *133*, 102−104.
(18) Loh, Y. Y.; Nagao, K.; Hoover, A. J.; Hesk, D.; Rivera, N. R.; Colletti, S. L.; Davies, I. W.; MacMillan, D. W. C. Photoredox-catalyzed deuteration and tritiation of pharmaceutical compounds. *Science* **2017**, *358*, 1182−1187.
(19) Palmer, W. N.; Chirik, P. J. Cobalt-Catalyzed Stereoretentive Hydrogen Isotope Exchange of C(sp^3)−H Bonds. *ACS Catal.* **2017**, *7*, 5674−5678.
(20) Chang, Y.; Yesilcimen, A.; Cao, M.; Zhang, Y.; Zhang, B.; Chan, J. Z.; Wasa, M. Catalytic Deuterium Incorporation within Metabolically Stable β-Amino C−H Bonds of Drug Molecules. *J. Am. Chem. Soc.* **2019**, *141*, 14570−14575.
(21) Neubert, L.; Michalik, D.; Bähn, S.; Imm, S.; Neumann, H.; Atzrodt, J.; Derdau, V.; Holla, W.; Beller, M. Ruthenium-Catalyzed Selective α,β-Deuteration of Bioactive Amines. *J. Am. Chem. Soc.* **2012**, *134*, 12239−12244.
(22) Li, W.; Rabeah, J.; Bourriquen, F.; Yang, D.; Kreyenschulte, C.; Rockstroh, N.; Lund, H.; Bartling, S.; Surkus, A.-E.; Junge, K.; Brückner, A.; Lei, A.; Beller, M. Scalable and selective deuteration of (hetero)arenes. *Nat. Chem.* **2022**, *14*, 334−341.
(23) Atzrodt, J.; Derdau, V.; Kerr, W. J.; Reid, M. C−H Functionalisation for Hydrogen Isotope Exchange. *Angew. Chem., Int. Ed.* **2018**, *57*, 3022−3047.
(24) Esaki, H.; Aoki, F.; Umemura, M.; Kato, M.; Maegawa, T.; Monguchi, Y.; Sajiki, H. Efficient H/D Exchange Reactions of Alkyl-Substituted Benzene Derivatives by Means of the Pd/C−H_2−D_2O System. *Chem. - Eur. J.* **2007**, *13*, 4052−4063.
(25) Hu, Y.; Liang, L.; Wei, W.-t.; Sun, X.; Zhang, X.-j.; Yan, M. A convenient synthesis of deuterium labeled amines and nitrogen heterocycles with KO*t*-Bu/DMSO-d_6. *Tetrahedron* **2015**, *71*, 1425−1430.
(26) Kopf, S.; Bourriquen, F.; Li, W.; Neumann, H.; Junge, K.; Beller, M. Recent Developments for the Deuterium and Tritium Labeling of Organic Molecules. *Chem. Rev.* **2022**, *122*, 6634−6718.
(27) Czeskis, B.; Elmore, C. S.; Haight, A.; Hesk, D.; Maxwell, B. D.; Miller, S. A.; Raglione, T.; Schildknegt, K.; Traverse, J. F.; Wang, P. Deuterated active pharmaceutical ingredients: A science-based proposal for synthesis, analysis, and control. Part 1: Framing the problem. *J. Labelled Comp. Radiopharm.* **2019**, *62*, 690−694.
(28) Garlets, Z. J.; Yuill, E. M.; Yang, A.; Ye, Q.; Ding, W.; Wood, C.; Fan, J.; Cuniere, N. L.; Sfouggatakis, C. Tracking the Isotopologues: Process Improvement for the Synthesis of a Deuterated Pyrazole. *Org. Process. Res. Dev.* **2023**, *27*, 159−166.
(29) Ofosu-Asante, K.; Stock, L. M. A convenient and selective method for reductive deuteration of aryl carbonyl compounds. *J. Org. Chem.* **1987**, *52*, 2938−2939.
(30) Galton, S. A.; Abbas, R. Deuterium isotope effect and migratory aptitudes in the Clemmensen reduction of 1-indanones. *J. Org. Chem.* **1973**, *38*, 2008−2011.
(31) Enzell, C. R. Deuterium labelling by Clemmensen reduction. *Tetrahedron Lett.* **1966**, *7*, 1285−1288.
(32) Ou, W.; Xiang, X.; Zou, R.; Xu, Q.; Loh, K. P.; Su, C. Room-Temperature Palladium-Catalyzed Deuterogenolysis of Carbon Oxygen Bonds towards Deuterated Pharmaceuticals. *Angew. Chem., Int. Ed.* **2021**, *60*, 6357−6361.
(33) Li, H.; Hou, Y.; Liu, C.; Lai, Z.; Ning, L.; Szostak, R.; Szostak, M.; An, J. Pentafluorophenyl Esters: Highly Chemoselective Ketyl Precursors for the Synthesis of α,α-Dideuterio Alcohols Using SmI_2 and D_2O as a Deuterium Source. *Org. Lett.* **2020**, *22*, 1249−1253.
(34) Luo, S.; Weng, C.; Ding, Y.; Ling, C.; Szostak, M.; Ma, X.; An, J. Reductive Deuteration of Aromatic Esters for the Synthesis of α,α-Dideuterio Benzyl Alcohols Using D_2O as Deuterium Source. *Synlett* **2021**, *32*, 51−56.
(35) Mo, X.; Yakiwchuk, J.; Dansereau, J.; McCubbin, J. A.; Hall, D. G. Unsymmetrical Diarylmethanes by Ferroceniumboronic Acid Catalyzed Direct Friedel−Crafts Reactions with Deactivated Benzylic Alcohols: Enhanced Reactivity due to Ion-Pairing Effects. *J. Am. Chem. Soc.* **2015**, *137*, 9694−9703.
(36) Taylor, R. D.; MacCoss, M.; Lawson, A. D. G. Rings in Drugs. *J. Med. Chem.* **2014**, *57*, 5845−5859.
(37) Vitaku, E.; Smith, D. T.; Njardarson, J. T. Analysis of the Structural Diversity, Substitution Patterns, and Frequency of Nitrogen Heterocycles among U.S. FDA Approved Pharmaceuticals. *J. Med. Chem.* **2014**, *57*, 10257−10274.
(38) Vang, Z. P.; Hintzsche, S. J.; Clark, J. R. Catalytic Transfer Deuteration and Hydrodeuteration: Emerging Techniques to Selectively Transform Alkenes and Alkynes to Deuterated Alkanes. *Chem. - Eur. J.* **2021**, *27*, 9988−10000.
(39) Espinal-Viguri, M.; Neale, S. E.; Coles, N. T.; Macgregor, S. A.; Webster, R. L. Room Temperature Iron-Catalyzed Transfer Hydrogenation and Regioselective Deuteration of Carbon−Carbon Double Bonds. *J. Am. Chem. Soc.* **2019**, *141*, 572−582.
(40) Linford-Wood, T. G.; Coles, N. T.; Webster, R. L. Room temperature iron catalyzed transfer hydrogenation using *n*-butanol and poly(methylhydrosiloxane). *Green Chem.* **2021**, *23*, 2703−2709.
(41) Li, L.; Hilt, G. Regiodivergent DH or HD Addition to Alkenes: Deuterohydrogenation versus Hydrodeuterogenation. *Org. Lett.* **2020**, *22*, 1628−1632.
(42) Walker, J. C. L.; Oestreich, M. Regioselective Transfer Hydrodeuteration of Alkenes with a Hydrogen Deuteride Surrogate Using $B(C_6F_5)_3$ Catalysis. *Org. Lett.* **2018**, *20*, 6411−6414.
(43) Li, L.; Hilt, G. Indium Tribromide-Catalysed Transfer-Hydrogenation: Expanding the Scope of the Hydrogenation and of the Regiodivergent DH or HD Addition to Alkenes. *Chem. - Eur. J.* **2021**, *27*, 11221−11225.
(44) Liu, R. Y.; Buchwald, S. L. CuH-Catalyzed Olefin Functionalization: From Hydroamination to Carbonyl Addition. *Acc. Chem. Res.* **2020**, *53*, 1229−1243.
(45) Wang, H.; Buchwald, S. L. Copper-Catalyzed, Enantioselective Hydrofunctionalization of Alkenes. *Org. React.* **2019**, 121−206.
(46) Zhu, S.; Niljianskul, N.; Buchwald, S. L. Enantio- and Regioselective CuH-Catalyzed Hydroamination of Alkenes. *J. Am. Chem. Soc.* **2013**, *135*, 15746−15749.
(47) Miki, Y.; Hirano, K.; Satoh, T.; Miura, M. Copper-Catalyzed Intermolecular Regioselective Hydroamination of Styrenes with Polymethylhydrosiloxane and Hydroxylamines. *Angew. Chem., Int. Ed.* **2013**, *52*, 10830−10834.
(48) Mohr, J.; Oestreich, M. Balancing C═C Functionalization and C═O Reduction in Cu−H Catalysis. *Angew. Chem., Int. Ed.* **2016**, *55*, 12148−12149.

https://doi.org/10.1021/jacsau.3c00053
JACS Au 2023, 3, 1583−1589

(49) Suess, A. M.; Lalic, G. Copper-Catalyzed Hydrofunctionalization of Alkynes. *Synlett* **2016**, *27*, 1165−1174.
(50) Mailig, M.; Hazra, A.; Armstrong, M. K.; Lalic, G. Catalytic Anti-Markovnikov Hydroallylation of Terminal and Functionalized Internal Alkynes: Synthesis of Skipped Dienes and Trisubstituted Alkenes. *J. Am. Chem. Soc.* **2017**, *139*, 6969−6977.
(51) Hazra, A.; Chen, J.; Lalic, G. Stereospecific Synthesis of *E*-Alkenes through Anti-Markovnikov Hydroalkylation of Terminal Alkynes. *J. Am. Chem. Soc.* **2019**, *141*, 12464−12469.
(52) Hazra, A.; Kephart, J. A.; Velian, A.; Lalic, G. Hydroalkylation of Alkynes: Functionalization of the Alkenyl Copper Intermediate through Single Electron Transfer Chemistry. *J. Am. Chem. Soc.* **2021**, *143*, 7903−7908.
(53) Cheng, L.-J.; Mankad, N. P. Cu-Catalyzed Hydrocarbonylative C−C Coupling of Terminal Alkynes with Alkyl Iodides. *J. Am. Chem. Soc.* **2017**, *139*, 10200−10203.
(54) Fujihara, T.; Semba, K.; Terao, J.; Tsuji, Y. Regioselective transformation of alkynes catalyzed by a copper hydride or boryl copper species. *Catal. Sci. Technol.* **2014**, *4*, 1699−1709.
(55) Kortman, G. D.; Hull, K. L. Copper-Catalyzed Hydroarylation of Internal Alkynes: Highly Regio- and Diastereoselective Synthesis of 1,1-Diaryl, Trisubstituted Olefins. *ACS Catal.* **2017**, *7*, 6220−6224.
(56) Shi, S.-L.; Buchwald, S. L. Copper-catalysed selective hydroamination reactions of alkynes. *Nat. Chem.* **2015**, *7*, 38−44.
(57) Das, M.; Kaicharla, T.; Teichert, J. F. Stereoselective Alkyne Hydrohalogenation by Trapping of Transfer Hydrogenation Intermediates. *Org. Lett.* **2018**, *20*, 4926−4929.
(58) Semba, K.; Fujihara, T.; Xu, T.; Terao, J.; Tsuji, Y. Copper-Catalyzed Highly Selective Semihydrogenation of Non-Polar Carbon-Carbon Multiple Bonds using a Silane and an Alcohol. *Adv. Synth. Catal.* **2012**, *354*, 1542−1550.
(59) Korytiaková, E.; Thiel, N. O.; Pape, F.; Teichert, J. F. Copper(I)-catalysed transfer hydrogenations with ammonia borane. *Chem. Commun.* **2017**, *53*, 732−735.
(60) Whittaker, A. M.; Lalic, G. Monophasic Catalytic System for the Selective Semireduction of Alkynes. *Org. Lett.* **2013**, *15*, 1112−1115.
(61) Sloane, S. E.; Reyes, A.; Vang, Z. P.; Li, L.; Behlow, K. T.; Clark, J. R. Copper-Catalyzed Formal Transfer Hydrogenation/Deuteration of Aryl Alkynes. *Org. Lett.* **2020**, *22*, 9139−9144.
(62) Vang, Z. P.; Reyes, A.; Sonstrom, R. E.; Holdren, M. S.; Sloane, S. E.; Alansari, I. Y.; Neill, J. L.; Pate, B. H.; Clark, J. R. Copper-Catalyzed Transfer Hydrodeuteration of Aryl Alkenes with Quantitative Isotopomer Purity Analysis by Molecular Rotational Resonance Spectroscopy. *J. Am. Chem. Soc.* **2021**, *143*, 7707−7718.
(63) Mills, M. D.; Sonstrom, R. E.; Vang, Z. P.; Neill, J. L.; Scolati, H. N.; West, C. T.; Pate, B. H.; Clark, J. R. Enantioselective Synthesis of Enantioisotopomers with Quantitative Chiral Analysis by Chiral Tag Rotational Spectroscopy. *Angew. Chem., Int. Ed.* **2022**, *61*, e202207275.
(64) Cheng, L.-J.; Islam, S. M.; Mankad, N. P. Synthesis of Allylic Alcohols via Cu-Catalyzed Hydrocarbonylative Coupling of Alkynes with Alkyl Halides. *J. Am. Chem. Soc.* **2018**, *140*, 1159−1164.
(65) Fujihara, T.; Xu, T.; Semba, K.; Terao, J.; Tsuji, Y. Copper-Catalyzed Hydrocarboxylation of Alkynes Using Carbon Dioxide and Hydrosilanes. *Angew. Chem., Int. Ed.* **2011**, *50*, 523−527.
(66) Brechmann, L. T.; Teichert, J. F. Catch It If You Can: Copper-Catalyzed (Transfer) Hydrogenation Reactions and Coupling Reactions by Intercepting Reactive Intermediates Thereof. *Synthesis* **2020**, *52*, 2483−2496.
(67) Liu, S.; Liu, J.; Wang, Q.; Wang, J.; Huang, F.; Wang, W.; Sun, C.; Chen, D. The origin of regioselectivity in Cu-catalyzed hydrocarbonylative coupling of alkynes with alkyl halides. *Org. Chem. Front.* **2020**, *7*, 1137−1148.
(68) Reyes, A.; Torres, E. R.; Vang, Z. P.; Clark, J. R. Highly Regioselective Copper-Catalyzed Transfer Hydrodeuteration of Unactivated Terminal Alkenes. *Chem. - Eur. J.* **2022**, *28*, e202104340.
(69) Christiansen, E.; Due-Hansen, M. E.; Urban, C.; Merten, N.; Pfleiderer, M.; Karlsen, K. K.; Rasmussen, S. S.; Steensgaard, M.; Hamacher, A.; Schmidt, J.; Drewke, C.; Petersen, R. K.; Kristiansen, K.; Ullrich, S.; Kostenis, E.; Kassack, M. U.; Ulven, T. Structure-Activity Study of Dihydrocinnamic Acids and Discovery of the Potent FFA1 (GPR40) Agonist TUG-469. *ACS Med. Chem. Lett.* **2010**, *1*, 345−349.
(70) Stuetz, A.; Georgopoulos, A.; Granitzer, W.; Petranyi, G.; Berney, D. Synthesis and Structure-Activity Relationships of Naftifine-Related Allylamine Antimycotics. *J. Med. Chem.* **1986**, *29*, 112−125.
(71) Cazzola, M.; Testi, R.; Matera, M. G. Clinical Pharmacokinetics of Salmeterol. *Clin. Pharmacokinet.* **2002**, *41*, 19−30.
(72) Smith, J. A.; Wilson, K. B.; Sonstrom, R. E.; Kelleher, P. J.; Welch, K. D.; Pert, E. K.; Westendorff, K. S.; Dickie, D. A.; Wang, X.; Pate, B. H.; Harman, W. D. Preparation of cyclohexene isotopologues and stereoisotopomers from benzene. *Nature* **2020**, *581*, 288−293.
(73) Pérez, C.; Lobsiger, S.; Seifert, N. A.; Zaleski, D. P.; Temelso, B.; Shields, G. C.; Kisiel, Z.; Pate, B. H. Broadband Fourier transform rotational spectroscopy for structure determination: The water heptamer. *Chem. Phys. Lett.* **2013**, *571*, 1−15.
(74) Balle, T. J.; Flygare, W. H. Fabry−Perot cavity pulsed Fourier transform microwave spectrometer with a pulsed nozzle particle source. *Rev. Sci. Instrum.* **1981**, *52*, 33−45.

https://doi.org/10.1021/jacsau.3c00053
JACS Au 2023, 3, 1583−1589